Pramāṇa, Vol. 23, No. 4, October 1984, pp. 475–484. © Printed in India.

Zeros of the helicity amplitudes of $\Sigma^- - p$ and $\Lambda - p$ elastic scattering

S MOHANTY and J K MOHAPATRA*

Department of Physics, Utkal University, Vani Vihar, Bhubaneswar 751 004, India
* Department of Physics, Regional College of Education, Bhubaneswar 751 007, India

MS received 16 January 1984; revised 14 June 1984

Abstract. The forces of interaction as reflected in the $\cos\theta$ plane analytic structures of the helicity amplitudes of $\Sigma^- - p$ and $\Lambda - p$ scattering are optimally exploited using the conformal mapping technique of Cutkosky and coworkers. A suitable parametrization of these amplitudes in the mapped variable is then chosen so that it can see the zeros better. These zeros are then located by making a good fit to the differential scattering cross-section curves. The effect of these zeros upon the cross-sections is discussed. Values for the phase shifts and coupling parameters between channels of fixed J values are also computed.

Keywords. $\Sigma^- - p$ elastic scattering; $\Lambda - p$ elastic scattering; analyticity; conformal mapping; optimised polynomial expansion technique.

PACS No. 13·75 Ev.

1. Introduction

Very little is known about the hyperon proton interactions, primarily because of the brief life of hyperon (Hauptman 1977) which corresponds to decay path lengths of a few centimetre for hyperon momenta of several GeV/C. This absence of data has made the progress in theoretical studies of scattering rather slow. A few authors (deSwart and Dullemond 1961; deSwart and Iddings 1962; Lettessier and Tounsi 1971; Nagels *et al* 1977, 1979) have dealt with this scattering using different potential models and have carried out phase shift analysis and total cross-section calculations. However, no effort has been made to locate and study the zeros of the helicity amplitudes of this scattering process, although in the absence of nearby poles, zeros other than the kinematical zeros, can be considered to be interesting features of the amplitudes for study. In this paper we attempt to locate these zeros using the optimised polynomial expansion technique (OPET) of Cutkosky and Deo (1968) and Ciulli (1969) and study their movement with energy. The OPET is based on the conformal mapping prescriptions of Nehari (1952). This technique has the greater capacity of information storage in the $\cos\theta$ plane as has been demonstrated by earlier workers (Chao 1970; Shih 1971; Deo and Mohapatra 1982) for different scattering processes.

We map the cut $\cos\theta$ plane of analyticity of the helicity amplitudes into the interior of an ellipse. Then parametrizing the amplitudes suitably and using the χ^2-minimization technique the position of the zeros which provide a possible explanation for the minima observed in the differential scattering cross-section curve of $\Sigma^- - p$ and $\Lambda - p$ scatterings are located. These zeros are found to move with energy.

Section 2 gives our scheme of parametrization. Section 3 gives the results and concluding remarks.

2. Scheme of parametrization

For the scatterings

$$\Sigma^- - p \to \Sigma^- - p$$
$$\Lambda - p \to \Lambda - p$$

the scattering amplitude has six independent helicity amplitudes (Lettessier and Tounsi 1972) given by

$$\Phi_1 = \langle +\tfrac{1}{2} +\tfrac{1}{2}|\phi|+\tfrac{1}{2}+\tfrac{1}{2}\rangle = \frac{1}{2K_H}\sum_J (2J+1)\phi_1^J d_{00}^J(\theta), \tag{1}$$

$$\Phi_2 = \langle +\tfrac{1}{2} +\tfrac{1}{2}|\phi|-\tfrac{1}{2}-\tfrac{1}{2}\rangle = \frac{1}{2K_H}\sum_J (2J+1)\phi_2^J d_{00}^J(\theta), \tag{2}$$

$$\Phi_3 = \langle +\tfrac{1}{2} -\tfrac{1}{2}|\phi|+\tfrac{1}{2}-\tfrac{1}{2}\rangle = \frac{1}{2K_H}\sum_J (2J+1)\phi_3^J d_{11}^J(\theta), \tag{3}$$

$$\Phi_4 = \langle +\tfrac{1}{2} -\tfrac{1}{2}|\phi|-\tfrac{1}{2}+\tfrac{1}{2}\rangle = \frac{1}{2K_H}\sum_J (2J+1)\phi_4^J d_{11}^J(\theta), \tag{4}$$

$$\Phi_5 = \langle +\tfrac{1}{2} +\tfrac{1}{2}|\phi|+\tfrac{1}{2}-\tfrac{1}{2}\rangle = \frac{1}{2K_H}\sum_J (2J+1)\phi_5^J d_{10}^J(\theta), \tag{5}$$

$$\Phi_6 = \langle +\tfrac{1}{2} +\tfrac{1}{2}|\phi|-\tfrac{1}{2}+\tfrac{1}{2}\rangle = \frac{1}{2K_H}\sum_J (2J+1)\phi_6^J d_{10}^J(\theta), \tag{6}$$

where

ϕ_i^J is the partial helicity amplitude; K_H the momentum of the particular hyperon; $d^J_{\lambda'\lambda}$ the reduced rotation matrix; $\lambda = \lambda_p - \lambda_H$; $\lambda' = \lambda'_p - \lambda'_H$; λ_p is the helicity of incoming proton; λ'_p the helicity of outgoing proton; λ'_H the helicity of the particular incoming hyperon and λ'_H the helicity of the particular outgoing hyperon.

In terms of the partial helicity amplitudes, the differential scattering cross-section is given by (Lettessier and Tounsi 1971),

$$\frac{d\sigma}{d\Omega} = \frac{\alpha}{2K_H^2}\sum_{i=1}^{6}\sum_{J=0}^{\infty}\sum_{J'=0}^{\infty}(2J+1)(2J'+1)(-1)^{\lambda-\lambda'}(\delta_{i5}+\delta_{i6}+1)$$
$$\times \phi_i^J \phi_i^{J'^*}\sum_l \langle JJ',\lambda'-\lambda|10\rangle\langle JJ',\lambda'-\lambda|10\rangle P_l(\cos\theta), \tag{7}$$

where $$\alpha = 1/(2S_H+1)(2S_p+1) = \text{the statistical weight}, \tag{8}$$

S_H is the spin of the hyperon and S_p the spin of the proton.

The helicity amplitudes, Φ_i, have (Cohen-Tannoudji 1968) kinematical singularities in the form of zeros at $\cos\theta = \pm 1$, because they can be written as

$$\Phi_i = f_{\lambda\lambda'}\Phi'_i, \tag{9}$$

where $$f_{\lambda\lambda'} = (1+\cos\theta)^{|\lambda+\lambda'|/2}(1-\cos\theta)^{|\lambda-\lambda'|/2}. \tag{10}$$

However, these singularities do not affect (Cohen-Tannoudji 1968; Szego 1959) their domain of convergence which is completely characterized by the dynamical singularities. We call Φ'_i as reduced helicity amplitudes.

The Φ_i''s for $\Sigma^- - p$ scattering are analytic in the $\cos\theta$ plane except for the cuts $x_{+\Sigma^-}$ to ∞ and $-x_{-\Sigma^-}$ to $-\infty$ (figure 1a), where

$$x_{+\Sigma^-} = 1 + 2M_p^2/K_{\Sigma^-}^2, \tag{11a}$$

$$-x_{-\Sigma^-} = -1 - (M_\Lambda + M_p)^2/2K_{\Sigma^-}^2, \tag{11b}$$

and similarly those of $\Lambda - p$ scattering are analytic in the $\cos\theta$ plane except for the cuts $x_{+\Lambda}$ to ∞ and $-x_{-\Lambda}$ to $-\infty$ (figure 1a) where

$$x_+ = 1 + 2M_p^2/K_\Lambda^2, \tag{12a}$$

$$-x_- = -1 - (M_{\bar{\Lambda}} + M_{\bar{p}})^2/2K_\Lambda^2. \tag{12b}$$

We symmetrize the cuts by mapping the x-plane onto the w-plane (figure 1b) in which the cuts run along ($-\infty$ to $-W$) and (W to ∞), where

$$W = (x_+ X_- + x_- X_+)/(X_+ + X_-), \tag{13}$$

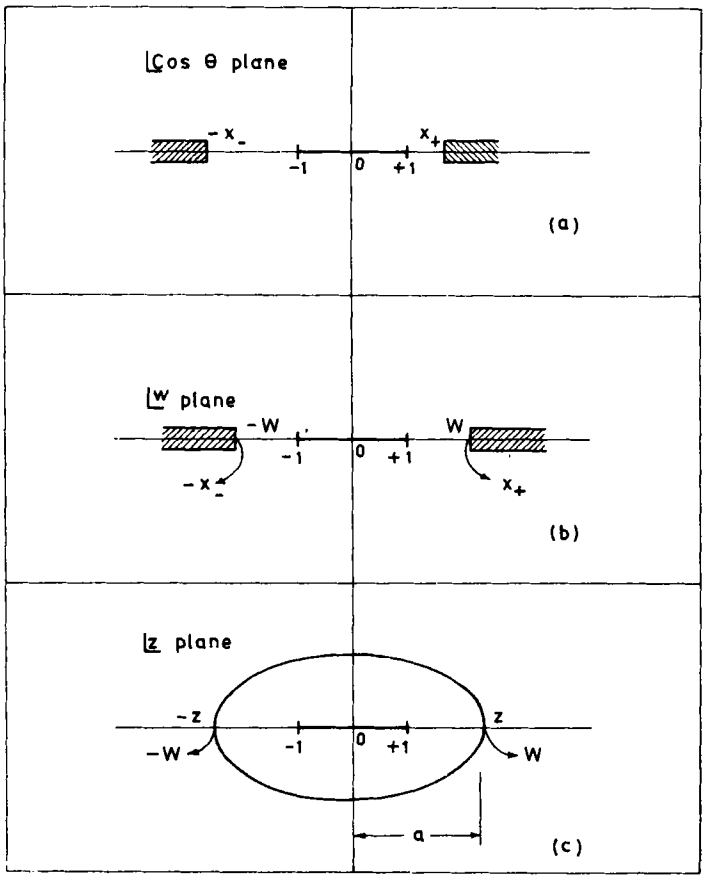

Figure 1. **a.** Analytic structure of the scattering amplitude in $\cos\theta$ plane. x_+ and $-x_-$ are the positions of the right hand and left hand cuts respectively. **b** Position of the symmetrized cuts in the w plane. **c.** Ellipse of convergence in the mapped z plane with semi major axis a.

and $$X_{\pm} = (x_{\pm}^2 - 1)^{1/2}. \tag{14}$$

The mapped w-plane is defined by

$$w = (x - x_0)/(1 - xx_0), \tag{15}$$

where $$x_0 = (x_- - x_+)/(x_+x_- + X_+X_- - 1). \tag{16}$$

The physical region $(-1, 1)$ in the x-plane is mapped onto the region $(-1, 1)$ of the w-plane. We then map the w-plane into an unifocal ellipse (figure 1c) in the z-plane such that $x = \pm 1$ maps into $z = \pm 1$, and the cuts are mapped to form the boundary of the ellipse. z is given by,

$$z = \sin\psi(w, k_0), \tag{17}$$

$$\psi(w, k) = \pi F(\sin^{-1} w, k)/2K(k), \tag{18}$$

where $F(\alpha, k)$ and $K(k) = F(\pi/2, k)$ are respectively the incomplete and complete elliptic integrals of the first kind and $k_0 = 1/W$. The mapping from the symmetrized w-plane to a unifocal ellipse is chosen because at low energies, this mapping tends to maximise the rate of convergence, given by

$$R = a + (a^2 - 1)^{1/2}, \tag{19}$$

a being the semimajor axis of the ellipse. This mapping has been effectively used by many authors (Chao 1971; Shih 1971; Deo 1982) for low energy data analysis of various scattering processes.

We now represent the six amplitudes, Φ_i's, as

$$\Phi_i' = \Phi_{iR}' + i\Phi_{iI}', \tag{20}$$

where Φ_{iR}' is the real part and Φ_{iI}' the imaginary part of the reduced helicity amplitudes. Assuming that there is at least one dynamical zero in each of these Φ_{iR}' and Φ_{iI}', we write them in the following polynomial form

$$\Phi_{iR}' = (z - z_{0R}^i) \sum_{n=0}^{\infty} a_{in} T_n(z), \tag{21}$$

and $$\Phi_{iI}' = (z - z_{0I}^i) \sum_{n=0}^{\infty} b_{in} T_n(z), \tag{22}$$

where $T_n(z)$ is the Chebyseff polynomial of order n, z_{0R} and z_{0I} are the positions of the zeros of the corresponding amplitudes. $T_n(z)$ is used in this expansion because its figure of convergence in an ellipse and coincides with the domain of analyticity of the amplitudes in the z-plane, and so a suitably truncated series will still be a faithful representation of the actual amplitudes in so far as the fit to the data is concerned.

3. Result and conclusion

After constructing the helicity amplitudes (21) and (22) as polynomials in the mapped z variable, the differential scattering cross-sections were calculated using (7) and was fitted to the data for $\Sigma^- - p$ scattering at 10 (Nagels *et al* 1977), 40 and 150 MeV and $\Lambda - p$ scattering at 100 MeV (deSwart and Dullemond (1961).

3.1 *Fit for Σ^-–p scattering*

After a preliminary blind search for the parameter in (21) and (22) to obtain a reliable fit to the Σ^-–p scattering differential cross-section data at 10, 40 and 150 MeV it was observed that either one has to introduce more number of zeros or consider a large number of terms of the polynomial expansion to obtain a tolerable fit to the data. This could possibly be due to the availability of only scanty, error affected data. In the final analysis at least two zeros had to be introduced in each of the reduced helicity amplitudes which were then written as

$$\Phi'_{iR} = (z - z_{0R}^{i1})(z - z_{0R}^{i2}) \sum_{n=0}^{\infty} a_{in} T_n(z), \tag{23}$$

and

$$\Phi'_{il} = (z - z_{0I}^{i1})(z - z_{0I}^{i2}) \sum_{n=0}^{\infty} b_{in} T_n(z). \tag{24}$$

The helicity amplitudes were easily computed using (9). The best fit was obtained with just the constant terms of (23) and (24). For all the three energies considered $\chi^2/\text{NDF} < 1$. Table 1 gives the position of the zeros, Z_{0R}^{im} and Z_{0I}^{im}, $m = 1, 2, \ldots$. It is seen that the second zeros of all the Φ'_{iR} and Φ'_{il} are buried deep in the unphysical region. Although a few of these second zeros seem to have rapid movements, it is difficult to predict definitely the energy at which they cross the physical domain. However most of the first zeros at all the three energies are in the physical region except those of Φ'_{1R} and Φ'_{2R} which move into the physical region as the energy is increased, and those of Φ'_{5I} and Φ'_{6I} which move out into the unphysical region as the energy is increased.

3.2 *Fit for Λ–p scattering*

A fit to the Λ–p scattering differential cross-section data at 100 MeV demonstrated some interesting features in that for a reliable fit to the data it was necessary to introduce a second zero in the expansion for all the Φ'_{iR}, and the reduced helicity amplitudes are written as

Table 1. Position of zeros (in radian) for Σ^-–p scattering.

Reduced helicity amplitudes	Zeros	Z_0^{i1} (MeV)			Z_0^{i2} (MeV)		
		10	40	150	10	40	150
Φ'_{1R}		−1·86	−0·75	−0·90	3·86	5·06	24·07
Φ'_{2R}		1·41	0·24	0·16	−1·46	−2·84	−16·97
Φ'_{3R}		−0·68	−0·77	−0·91	3·24	4·06	68·29
Φ'_{4R}		−0·50	−0·66	−0·76	5·1	4·35	−34·02
Φ'_{5R}		0·56	−0·04	−0·10	27·45	15·61	15·15
Φ'_{6R}		0·12	−0·06	−0·12	−17·05	−6·74	15·76
Φ'_{1I}		0·41	0·70	1·0	−3·68	−2·27	−28·01
Φ'_{2I}		0·36	0·70	1·0	−4·57	−2·26	−27·41
Φ'_{3I}		−0·29	−0·78	−0·93	4·46	3·09	−45·90
Φ'_{4I}		−0·03	−0·81	−0·95	6·97	3·57	−23·35
Φ'_{5I}		0·07	−0·56	−1·59	5·31	2·75	3·46
Φ'_{6I}		−0·005	−0·59	−4·18	4·69	3·10	10·44

$$\Phi'_{iR} = (z - z_{0R}^{i1})(z - z_{0R}^{i2}) \sum_{n=0}^{\infty} a_{in} T_n(z), \tag{25}$$

and

$$\Phi'_{il} = (z - z_{0l}^{i1}) \sum_{n=0}^{\infty} b_{in} T_n(z). \tag{26}$$

Here also all the second zeros are located in the unphysical region. Except Φ'_{3I} and Φ'_{4I} the other four Φ'_{il}s have their zeros in the unphysical region. The first zeros for Φ'_{5R} and Φ'_{6R} are at positive z-values, for Φ'_{1R}, Φ'_{2R}, Φ'_{3R} they are at negative z values and for Φ'_{4R} it is again in the unphysical region as shown in table 2. Here also $\chi^2/\text{NDF} < 1$.

The preponderence of the physical zeros in the backward angles for $\Sigma^- - p$ scattering at 10, 40 and 150 MeV provides possible explanation for the flat minima in the differential cross-section data for those angles. Most of the physical zeros move with energy, but the movement is so slow that these zeros perhaps get stabilised at higher energies. On the other hand in $\Lambda - p$ scattering at 100 MeV because two of these physical zeros are still there for positive z values and Φ'_{1I}, Φ'_{2I} and Φ'_{4R} do not have any zero in the physical region, the differential cross-section data though shows some form of a minimum still does not exhibit any flat minimum similar to those seen in $\Sigma^- - p$ scattering. Definite comments about the movement of the zeros of the $\Lambda - p$ scattering can perhaps be given only when reliable data at intermediate energies will be available. As we have made optimal use of the analytic structure of the helicity amplitudes we hope that the location of the zeros as determined by us is not dependent upon the specific parametrization chosen in this study.

We also tried to get the phase shifts and coupling parameters from our representation of the helicity amplitudes. Exploiting the orthogonality property of the reduced rotation matrix (Jacob 1959) *i.e.*

$$\int_0^{\pi} \sin\theta \, d^J_{\lambda'\lambda}(\theta) \, d^{J'}_{\lambda'\lambda}(\theta) \, d\theta = (2/2J+1)\delta_{JJ'}, \tag{27}$$

the partial helicity amplitudes are calculated for different J values. The R matrix was then computed using the following equation

Table 2. Position of zeros (in radian) for $\Lambda - p$ scattering.

Reduced helicity Amplitudes	Zeros	100 MeV	
		Z_0^{i1}	Z_0^{i2}
Φ'_{1R}		−0·1	−3·5
Φ'_{2R}		−0·05	−8·7
Φ'_{3R}		−0·5	−4·8
Φ'_{4R}		−1·4	−4·6
Φ'_{5R}		0·63	−28·9
Φ'_{6R}		0·63	−29·4
Φ'_{1I}		1·9	—
Φ'_{2I}		1·9	—
Φ'_{3I}		−0·84	—
Φ'_{4I}		−0·68	—
Φ'_{5I}		−17·8	—
Φ'_{6I}		− 1·6	—

$$\begin{vmatrix} R_1^J \\ R_2^J \\ R_3^J \\ R_4^J \\ R_5^J \\ R_6^J \end{vmatrix} = \begin{vmatrix} 1 & -1 & 0 & 0 & 0 & 0 \\ 0 & 0 & 1 & -1 & 0 & 0 \\ 0 & 0 & 0 & 0 & 1 & -1 \\ \frac{J}{2J+1} & \frac{J}{2J+1} & \frac{J+1}{2J+1} & \frac{J+1}{2J+1} & \frac{[J(J+1)]^{1/2}}{2J+1} & \frac{[J(J+1)]^{1/2}}{2J+1} \\ \frac{J+1}{2J+1} & \frac{J+1}{2J+1} & \frac{J}{2J+1} & \frac{J}{2J+1} & -\frac{[J(J+1)]^{1/2}}{2J+1} & -\frac{[J(J+1)]^{1/2}}{2J+1} \\ -\frac{[J(J+1)]^{1/2}}{2J+1} & -\frac{[J(J+1)]^{1/2}}{2J+1} & \frac{[J(J+1)]^{1/2}}{2J+1} & \frac{[J(J+1)]^{1/2}}{2J+1} & -\frac{1}{2J+1} & -\frac{1}{2J+1} \end{vmatrix} \begin{vmatrix} \phi_1^J \\ \phi_2^J \\ \phi_3^J \\ \phi_4^J \\ \phi_5^J \\ \phi_6^J \end{vmatrix} \tag{28}$$

where R_1^J gives the transitions in the singlet states with $l = J$, R_2^J the transitions in the triplet states with $l = J$, R_3^J the transitions between singlet and triplet states with $l = J$ and R_4^J, R_5^J, R_6^J the transitions between triplet states with $l \neq J$.

The R^J matrix is related to the scattering matrix S^J, which is symmetrical and unitary, by the following relation.

$$\langle \lambda_H' \lambda_p' | S^J | \lambda_H \lambda_p \rangle - \delta_{\lambda_H' \lambda_p' \lambda_H \lambda_p} = i \langle \lambda_H' \lambda_p' | R^J | \lambda_H \lambda_p \rangle. \tag{29}$$

This symmetric and unitary matrix S^J is characterised by $n(n+1)/2$ real parameters (Lettessier and Tounsi 1971), where the n value depends upon the number of coupled channels excited at any particular energy. Being symmetric and unitary it can be diagonalised by a real unitary matrix U:

$$S = U^{-1} \Delta U, \tag{30}$$

where
$$\Delta_{jj} = \exp[2i\delta_j], \tag{31}$$

and δ_j are the real eigen phase shifts which account for n real parameters. The other $n(n-1)/2$ parameters are used to characterise the matrix U. These $n(n-1)/2$ parameters define the coupling between various channels. For $n = 2$, U takes a particularly simple form (deSwart and Dullemond 1961; Lettessier and Tounsi 1971)

$$U = \begin{vmatrix} \cos\varepsilon & \sin\varepsilon \\ -\sin\varepsilon & \cos\varepsilon \end{vmatrix}, \tag{32}$$

where ε is the coupling parameter.

In passing we note that the eigen phase shifts are labelled by well-defined values of J, l and $2S+1$. Thus the phase shift corresponding to $S = 0$, $l = 1$, $J = l$ is designated by $^1P_1$, and that for $S = 1$, $l = 1$ and $J \neq 1$ by $3S_1$. Similarly the coupling parameter is labelled by definite S and l values *e.g.* the coupling between the channels with $S = 0$, $l = 1$ for $J = l$ is denoted by $^1\varepsilon_1$ and that for $S = l$, $l = 1$ for $J \neq l$ by $^3\varepsilon_1$. The phase shifts and coupling parameters thus obtained for $\Sigma^- - p$ scatterings at 10, 40 and 150 MeV Σ^- laboratory energy and for $\Lambda - p$ scattering at 100 MeV Λ laboratory energy are given in tables 3a, b and 4a, b. Our values for $\Lambda - p$ scattering agree well with those of earlier workers (deSwart 1961; Nagels 1977, 1979). Our $^3P_0$ phase shift value for $\Lambda - p$ scattering differs from those of earlier workers but agrees well with the result of Lettessier and Tounsi (1971). We have considered the coupling between the singlet and triplet phase shifts as was done by Lettessier and Tounsi (1971), and these are given in

Table 3a. Phase shifts and coupling parameters (in degrees) ($J = l$).

Phase shifts and coupling parameters of $\Sigma^- - p$ scattering	10 MeV	40 MeV	150 MeV
$^1S_0$	19·6	12·9	27·9
$^3P_0$	34·6	25·3	31·8
$^1P_0$	5·2	10·5	20·8
$^1\varepsilon_1$	−1·6	−0·25	−0·07
$^3P_1$	−7·9	−12·6	−24·0
$^1D_2$	−0·33	0·35	0·76
$^1\varepsilon_2$	−9·2	−0·83	−0·45
$^3D_2$	−0·17	−0·76	−2·7
$^1F_3$	−0·001	−0·002	−0·003
$^1\varepsilon_3$	2·2	2·5	0·009
$^3F_3$	0·64	1·1	0·46
$^1G_4$	0·00002	−0·00002	0·00008
$^1\varepsilon_4$	−0·002	−0·009	0·012
$^3G_4$	−0·22	−0·33	−0·18

Table 3b. Phase shifts and coupling parameters (in degrees) ($J \neq l$).

Phase shifts and coupling parameters of $\Sigma^- - p$ scattering	10 MeV	40 MeV	150 MeV
$^3S_1$	−6·4	−9·3	−17·4
$^3\varepsilon_1$	27·0	35·8	37·1
$^3D_1$	−1·0	1·2	3·0
$^3P_2$	−0·34	−1·1	0·38
$^3\varepsilon_2$	3·3	10·6	−35·4
$^3F_2$	−1·7	−3·0	−5·4
$^3D_3$	0·11	0·47	−0·41
$^3\varepsilon_3$	38·0	39·0	30·7
$^3G_3$	−0·0005	−0·002	0·013
$^3F_4$	0·22	0·18	0·22
$^3\varepsilon_4$	41·8	41·7	41·8
$^3H_4$	−0·00002	−0·0002	0·0001

Table 4a. Phase shifts and coupling parameters (in degrees) ($J = l$).

Phase shifts and coupling parameters of Λ–p scattering	Present analysis (100 MeV)	deSwart *et al* (1961) (100 MeV)	Nagels *et al* (1977) (106·9 MeV)	Nagels *et al* (1979) (106·9 MeV)
$^1S_0$	10·2	24·4	8·26	12·38
$^3P_0$	12·0	−4·6	−1·39	−2·82
$^1P_1$	10·7	13·0	9·03	−4·44
$^1\varepsilon_1$	0·007	—	—	—
$^3P_1$	8·3	9·5	0·45	−2·19
$^1D_2$	1·2	0·6	2·39	1·95
$^1\varepsilon_2$	0·23	—	—	—
$^3D_2$	1·7	1·7	2·44	2·28
$^1F_3$	0·002	—	0·10	0·01
$^1\varepsilon_3$	0·24	—	—	—
$^3F_3$	0·3	0·2	0·16	0·1
$^1G_4$	0·0002	—	—	—
$^1\varepsilon_4$	0·0003	—	—	—
$^3G_4$	−0·16	—	—	—

Table 4b. Phase shifts and coupling parameters (in degrees) ($J \neq l$).

Phase shifts and coupling parameters of Λ–p scattering	Present analysis (100 MeV)	deSwart *et al* (1961) (100 MeV)	Nagels *et al* (1977) (106·9 MeV)	Nagels *et al* (1979) (106·9 MeV)
$^3S_1$	−7·4	−17·5	16·57	12·49
$^3\varepsilon_1$	−33·2	−10·7	5·46	−1·82
$^3D_1$	5·9	2·1	1·88	7·39
$^3P_2$	3·8	9·7	8·72	6·14
$^3\varepsilon_2$	3·7	3·1	−0·25	−0·28
$^3F_2$	−0·77	—	0·21	0·24
$^3D_3$	0·21	1·7	1·85	1·6
$^3\varepsilon_3$	7·1	3·5	0·13	0·1
$^3G_3$	−0·009	—	—	—
$^3F_4$	0·17	0·1	0·25	0·20
$^3\varepsilon_4$	41·7	12·3	—	—
$^3H_4$	−0·00004	—	—	—

table 4a. The values of the phase shifts and coupling parameters of Σ^-–p scattering have now been reported for the first time. An out and out phase shift analysis of Σ^-–p scattering is in progress to check the correctness of the present values by analysing the position of zeros of the helicity amplitudes.

Acknowledgements

One of the authors thanks UGC India for a fellowship. They are also grateful to the Computer Centre of Utkal University for computation. Thanks are extended to Prof. B B Deo for helpful discussions.

References

Chao Y A 1970 *Phys. Rev. Lett.* **25** 309
Ciulli S 1969a *Nuovo Cimento* **A61** 787
Ciulli S 1969b *Nuovo Cimento* **A62** 301
Cutkosky R E and Deo B B 1968 *Phys. Rev.* **174** 1859
Cutkosky R E 1969 *Ann. Phys.* **54** 110
Cohen-Tannoudji G, Morel A and Navelet H 1968 *Ann. Phys.* **46** 239
Deo B B and Mohapatra J K 1982 *Pramana* **1** 39
deSwart J J and Dullemond C 1961 *Ann. Phys.* **16** 203
deSwart J J and Iddings C K 1962 *Phys. Rev.* **B12** 2810
Hauptman J M 1977 *Nucl. Phys.* **B125** 29
Jacob M and Wick G C 1959 *Ann. Phys.* **7** 404
Lettessier J and Tounsi A 1971 *Nuovo Cimento* **A65** 56
Nagels M M, Rijken T A and deSwart J J 1977 *Phys. Rev.* **D15** 2547
Nagels M M, Rijken T A and deSwart J J 1979 *Phys. Rev.* **D20** 1633
Nehari J 1952 *Conformal mapping* (New York: McGraw-Hill)
Shih C C 1971 *Phys. Rev.* **D4** 3293
Sezgo G 1959 *Orthogonal polynomials* American Physical Society **23**